



Development of Real-Time, In-pile Creep Test Rigs for Characterizing the Structural Materials of Nuclear Components

September 2021

Malwina A. Wilding, Michael McMurtrey, Anthony Crawford, Wesley Jones,
Hollis Kristopher Woodbury, and Kory Manning

Idaho National Laboratory



*INL is a U.S. Department of Energy National Laboratory
operated by Battelle Energy Alliance, LLC*

DISCLAIMER

This information was prepared as an account of work sponsored by an agency of the U.S. Government. Neither the U.S. Government nor any agency thereof, nor any of their employees, makes any warranty, expressed or implied, or assumes any legal liability or responsibility for the accuracy, completeness, or usefulness, of any information, apparatus, product, or process disclosed, or represents that its use would not infringe privately owned rights. References herein to any specific commercial product, process, or service by trade name, trade mark, manufacturer, or otherwise, does not necessarily constitute or imply its endorsement, recommendation, or favoring by the U.S. Government or any agency thereof. The views and opinions of authors expressed herein do not necessarily state or reflect those of the U.S. Government or any agency thereof.

Development of Real-Time, In-pile Creep Test Rigs for Characterizing the Structural Materials of Nuclear Components

**Malwina A. Wilding, Michael McMurtrey, Anthony Crawford, Wesley Jones, Hollis
Kristopher Woodbury, and Kory Manning
Idaho National Laboratory**

September 2021

**Idaho National Laboratory
Idaho Falls, Idaho 83415**

<http://www.inl.gov>

**Prepared for the
U.S. Department of Energy
Office of Nuclear Energy
Under DOE Idaho Operations Office
Contract DE-AC07-05ID14517**

Page intentionally left blank

ABSTRACT

New and improved materials are being considered for supporting both existing and next-generation nuclear reactors. Reactor materials can significantly degrade with time, thus limiting or altering their properties in harsh reactor environments. To accurately understand such material degradation, real-time data obtained under prototypic irradiation conditions are required. In particular, understanding the creep behavior of materials exposed to irradiation and elevated temperatures is essential for safety concern evaluations. To provide these capabilities, Idaho National Laboratory (INL)'s High Temperature Test Laboratory (HTTL) developed several instrumented test rigs for obtaining real-time data from specimens in well-controlled pressurized-water reactor (PWR) coolant conditions at the Materials Test Reactor. This technical report focuses on INL's efforts to evaluate and enhance the former creep test rig prototype that relied on linear variable differential transformers in laboratory settings. Specifically, the test rig can detect changes in the length of creep specimens, which is useful for measuring thermal expansion and creep deformation.

Page intentionally left blank

ACKNOWLEDGEMENTS

This work was supported through the Nuclear Energy Enabling Technology (NEET) Advanced Sensor and Instrumentation (ASI) Program, under Department of Energy (DOE) Idaho Operations Office Contract Number DE-AC07-05ID14517. We also wish to thank Richard Skifton, Kurt Davis, and Eric Larsen for their technical contributions to this work.

Page intentionally left blank

CONTENTS

ABSTRACT.....	iii
ACKNOWLEDGEMENTS.....	v
ACRONYMS.....	x
1. INTRODUCTION.....	1
2. BACKGROUND.....	2
2.1 Creep Test Fundamentals.....	2
2.2 Linear Variable Differential Transformer.....	3
3. METHODS AND MATERIALS.....	4
3.1 Standard Creep Testing.....	4
3.2 Out-of-Pile Creep Test Rig.....	5
3.3 Materials.....	6
3.4 Creep Testing Specimens.....	7
3.5 Double Delta.....	7
4. CALIBRATION RESULTS.....	8
4.1 Autoclave Calibration.....	8
4.2 Creep Specimen Measurements.....	10
5. CREEP TESTING RESULTS.....	11
5.1 Standard Creep Testing.....	11
5.2 Standard Creep Specimens.....	13
5.3 Autoclave Creep Testing.....	14
6. CONCLUSION.....	15
7. FUTURE WORK.....	15
8. REFERENCES.....	15

FIGURES

Figure 1. Creep curve.....	2
Figure 2. LVDT read out (demodulation) = $(V_A - V_B)/(V_A + V_B)$	3
Figure 3. Schematic of a creep test [9].....	4
Figure 4. Standard creep test frame: (a) level arm weights; (b) direct load weights.....	5
Figure 5. Schematic of the in-pile variable load creep test rig in an autoclave [7].....	6
Figure 6. Standard creep specimen.....	7
Figure 7. Creep specimen for autoclave creep testing.....	7
Figure 8. Double Delta system.....	8
Figure 9. Calibration fixture for autoclave testing.....	9
Figure 10. Autoclave calibration testing using the NI DAQ system at 300°C.....	10
Figure 11. Creep curve for Al-6061 specimen #2.....	12
Figure 12. Creep curve for Al-6061 specimen #3.....	13
Figure 13. Al-6061 creep specimen #2 after standard creep testing at 325°C and 15.896 MPa....	13
Figure 14. Al-6061 creep specimen #3 after standard creep testing at 325°C and 15.896 MPa....	13
Figure 15. Autoclave creep curve for Al-6061 dumbbell specimen #1.....	14
Figure 16. Dumbbell specimen #1 after autoclave creep testing at 325°C and 15.896 MPa.....	15

TABLES

Table 1. Chemical composition for Aluminum 6061.....	6
Table 2. LVDT demodulation sensitivity at room temperature and 100, 200, 300°C.....	9
Table 3. All Al-6061 creep specimen measurements prior to creep testing.....	10
Table 4. Length measurements, before and after standard creep testing.....	14

EQUATIONS

Equation 1 – Larson-Miller parameter equationBookmark '_Toc83863698' is not defined within the document.

Equation 2 – LVDT voltage demodulation to dimension conversionBookmark '_Toc83863699' is not defined within the do

Page intentionally left blank

ACRONYMS

ATR	Advanced Test Reactor
DAQ	data acquisition
DOE	U.S. Department of Energy
HBWR	Halden Boiling Water Reactor
HTTL	High Temperature Test Laboratory
INL	Idaho National Laboratory
LVDT	linear variable differential transformer
NI	National Instruments
PIE	post-irradiation examination
PWR	pressurized-water reactor
TC	thermocouple

Page intentionally left blank

Development of Real-Time, In-pile Test Rigs for Characterizing Nuclear Components Structural Materials

1. INTRODUCTION

Successful implementation of advanced nuclear reactors significantly relies on the performance of nuclear fuels and structural materials under extreme irradiation conditions. It is extremely challenging to develop advanced materials that, in addition to withstanding high temperatures, high neutron flux/fluences, and cyclic variations of thermal stress, can also resist oxidation, corrosion, and radiation effects for over 60+ years of the nuclear plant's lifetime. Irradiation damage begins with the creation of primary knock-off atoms displaced by the incident high-energy particles. When these high-energy particles interact with a crystal lattice, defects occur (e.g., interstitials, vacancies, and impurities), and aggregation of these point defects can cause the formation of defect clusters (e.g., dislocation loops and voids). Irradiation-induced defects can spark changes in macroscopic properties, including radiation-induced hardening, embrittlement, creep, and void swelling. Thus, over time, irradiation can significantly degrade and limit material properties in a manner that directly affects the longevity and safety of current and future nuclear power plants [1].

Irradiation creep refers to the time-dependent strain that arises from the effects of irradiation and stress on the materials, even at low relatively low temperatures at which thermal creep does not occur. The time-dependent strain that occurs in the absence of irradiation is generally called thermal creep, and initiates at relatively high operating temperatures. The performance of fuel, cladding, and structural components is easily affected by dimensional instabilities caused by irradiation creep. Traditionally, such dimensional changes are determined by repeatedly irradiating a specimen to a certain displacement dose level for a specified period of time, then removing it from the reactor for post-irradiation examination (PIE). The time and labor required to remove, examine, and return irradiated samples for each measurement makes this process very expensive and time consuming. However, tests that feature in-pile measurements taken during irradiation can enable heightened control over experimental variables, more detailed results related to the phenomena of interest, and improved accuracy relative to non-instrumented tests. Such benefits motivate the ongoing efforts to measure creep behavior during in-pile irradiation. Real-time creep measurement during irradiation enables assessment of two sets of simultaneous phenomena. The first is the applied stress and displacement damage that act simultaneously under dynamic irradiation conditions, altering the magnitude and spatial distribution of defect accumulation and causing the deformation behavior to substantially differ from that seen in PIE. The second is the thermal condition of the real-time test, irreproducible during PIE without again affecting the material microstructure [2].

The Idaho National Laboratory (INL) creep test rig is based on a design developed for irradiation testing at the Halden Boiling Water Reactor (HBWR) in Norway. INL fabricated and tested an out-of-pile version of this creep test rig at the High Temperature Test Laboratory (HTTL) as part of the Nuclear Energy Enabling Technology's Advanced Sensor and Instrumentation program. This report summarizes the status of INL's efforts to include an in-pile creep testing capability for the Materials Test Reactor. The rig was designed with an externally pressurized bellows to load a tensile specimen coupled with a linear variable displacement transformer (LVDT) for detecting material creep. Such a demonstration would provide an important capability to Department of Energy Office of Nuclear Energy programs and their stakeholders, partially replacing those testing capabilities lost due to the termination of HBWR operations. This is particularly relevant in light of the current plans to install water loops in the Advanced Test Reactor (ATR) I-positions in order to mimic the lost Halden capabilities [3,4,5].

2. BACKGROUND

2.1 Creep Test Fundamentals

Creep is a very slow, time-dependent plastic deformation that occurs in materials subjected to a stress (or load) at relatively high temperatures. As a result, the material undergoes a time-dependent deformation (strain) that could be dangerous while the material is in service. Therefore, creep rupture tests are used to measure the limitations of the material prior to being used in service. A typical creep curve is shown in Figure 1.

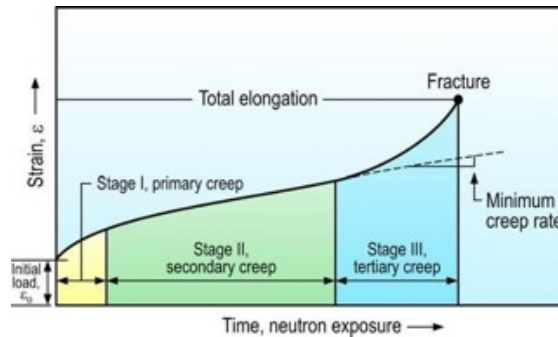


Figure 1. Creep curve.

In creep tests, temperature significantly impacts deformation phenomena by accelerating the microstructural defect rearrangements. This means that the temperature at which a given material begins to experience creep depends on its melting point. Generally, thermal creep for metals and alloys starts when the temperature of a material exceeds 0.3–0.4 times its melting temperature ($T > 0.3\text{--}0.4 T_m$). Primary creep (stage I) is associated with the period in which the creep rate decreases due to work hardening of the material. During this stage, initial hardening takes place, and the resistance to creep increases until secondary creep (stage II) begins. Secondary creep is associated with the period in which the creep rate remains roughly constant. Stage II creep is referred to as steady-state creep because a balance is achieved between the work hardening and annealing processes. The slope of the curve during stage II creep reflects the strain rate (i.e., creep rate) of the material. Tertiary creep (stage III) occurs when necking causes a reduction in the cross-sectional area, or when internal void formation causes an effective reduction in that same area. The creep rate increases due to the reduced cross section of the specimen and the associated increase in local stress. If stage III creep is allowed to continue, specimen fracture eventually occurs [6].

The Larson-Miller parameter is a widely used extrapolation method for predicting a material's service life. It can predict rupture lives with a given temperature and stress, and uses a correlative approach based on the Arrhenius rate equation (Equation (1)). The basic idea of the Larson-Miller parameter is to create a method to combine temperature and rupture life, and create models based on stress vs. Larson-Miller parameter to interpolate and extrapolate creep rupture lives at varying temperature and stress conditions.

Equation (1)

$$\text{LMP} = T(C + \log t_r)$$

T = temperature (K)

t_r = time before failure (hours)

C = material-specific constant

2.2 Linear Variable Differential Transformer

LVDTs are simple, reliable sensors that convert a specimen's mechanical movement into an electrical output. Figure 2 shows a simple schematic of how the LVDT design works. As indicated, a magnetically permeable core is attached to a specimen. The core then moves inside a tube in response to changes in the specimen's length or position. Three coils are wrapped around the tube: a single primary coil and two secondary coils [7].

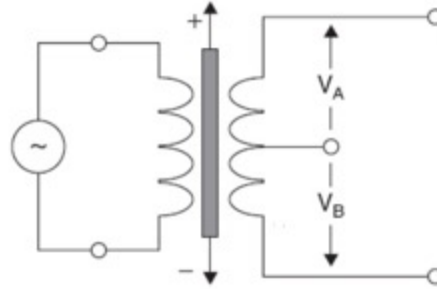


Figure 2. LVDT read out (demodulation) = $(V_A - V_B) / (V_A + V_B)$.

To operate the LVDT, an alternating (excitation) current is driven through the primary coil, inducing a voltage in each secondary coil. This voltage is proportional to its mutual inductance with the primary coil. As the specimen and attached core move, these mutual inductances shift, causing the voltages induced in the secondary coils to undergo a corresponding change. The secondary coils are connected in reverse series; an output voltage can be conveniently derived from the difference between the two secondary voltages. Specifically, when the core is in its central position (i.e., equidistant between the two secondary coils), equal but opposite voltages are induced in the secondary coils, making the output voltage zero. When the core is moved to its full-scale mechanical position (in either the positive or negative direction), the coil nearest the core goes full scale while the voltage in the other secondary coil drops to zero. Using the National Instruments (NI) data acquisition (DAQ) system, the primary coil is activated by a 5,000 Hz constant current generator, and the position of the core can be measured with an accuracy of $\pm 1 \mu\text{m}$. The LVDT voltage signal can be directly converted into a displacement value via Equation (2) below.

Equation (2)

$$\Delta X = S(\text{LVDT}_f - \text{LVDT}_i)$$

ΔX = change in displacement [mm]

S = sensitivity at a given temperature [mm / (V/V)], interpolated from calibration graph

LVDT_f = final demodulation reading [V/V]

LVDT_i = initial demodulation reading [V/V]

3. METHODS AND MATERIALS

3.1 Standard Creep Testing

Creep tests are conducted per the ASTM E139 standard [8], as they can be used to predict the service lives of materials prior to placing them into service. A standard creep test uses a tensile specimen that is placed under a constant stress, often by the simple method of suspending weights from it (direct load). Containing the specimen in a furnace whose temperature is controlled by a thermocouple (TC) attached to the gauge length of the specimen (Figure 3). The increase in length of the specimen is measured using a very sensitive extensometer and commercial LVDTs, since the actual amount of deformation prior to failure may be only 2 or 3%. The test results are then plotted on a graph of strain versus time to produce a curve such as the one illustrated in Figure 1 [9].

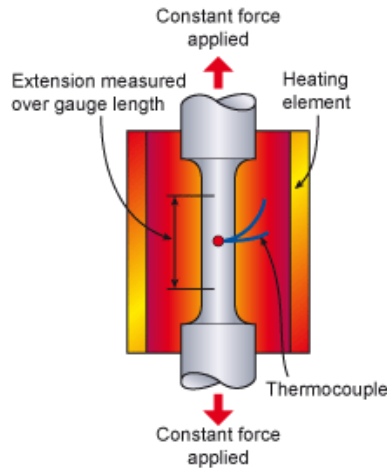


Figure 3. Schematic of a creep test [9].

An Applied Test Systems 2330 standard creep test frame was used, equipped with an Applied Test Systems Series 3210 furnace, temperature control systems, and calibrated load weights. The test specimen design was based on a standard tensile specimen, and the creep tests are generally carried out in air under atmospheric pressure. However, if creep data are needed for materials that react with air, this model may be used for testing in an enclosed chamber with an inert atmosphere, or in a vacuum. Also, depending on the load requirements, the standard creep testing apparatus can use either direct load weights (Figure 4[b]) or level arm weights (Figure 4[a]). For this experiment, all tests were conducted using direct load weights, an air environment surrounding the furnace, a high-sensitivity extensometer, and two LVDTs for accurate strain measurements.

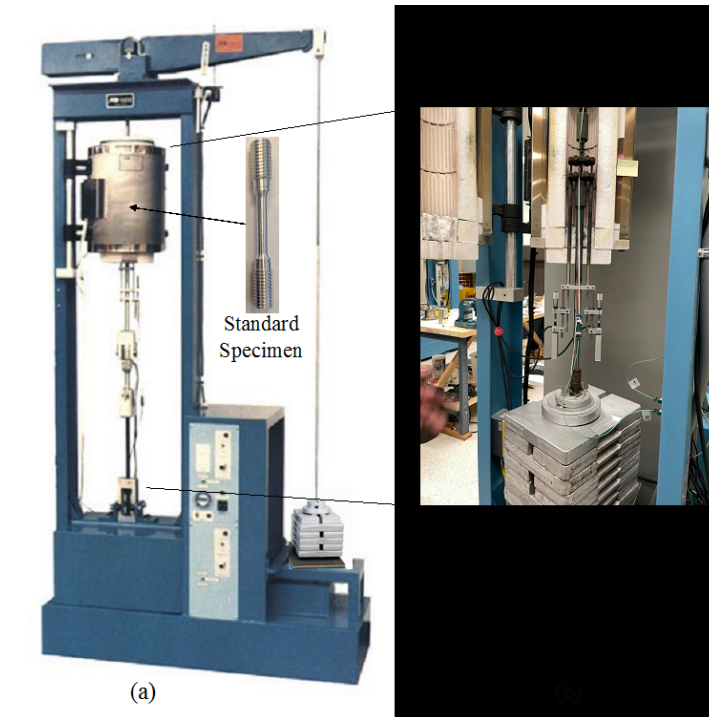


Figure 4. Standard creep test frame: (a) level arm weights; (b) direct load weights.

3.2 Out-of-Pile Creep Test Rig

The static creep test rig was initially developed for conducting specimen creep testing under pressurized-water reactor (PWR) prototypic conditions at HTTL to evaluate the performance of this design. The results of autoclave evaluations were used to finalize a test rig design for use in an ATR PWR loop [4]. The variable load creep test rig (Figure 5) was designed and fabricated for deployment in ATR Loop 2A. This test rig was a refinement of the aforementioned static creep test rig. Both creep test rig designs are comprised of several features, including a tensile specimen, an LVDT to measure dimensional changes, a static or variable load LVDT bellow assembly (7), a TC holder, a support structure to maintain the experiment in an in-pile environment, and an NI DAQ system for recording the LVDT and TC signals. Lastly, the fixture was designed to constrain the LVDT bellow assembly to one end of the specimen so that the bellows contraction places the specimen under tension. Cables extending from the LVDT and TC relay measurements of elongation and specimen temperature, respectively, and these properties are monitored by the NI DAQ system in real-time throughout the irradiation or autoclave testing [7].

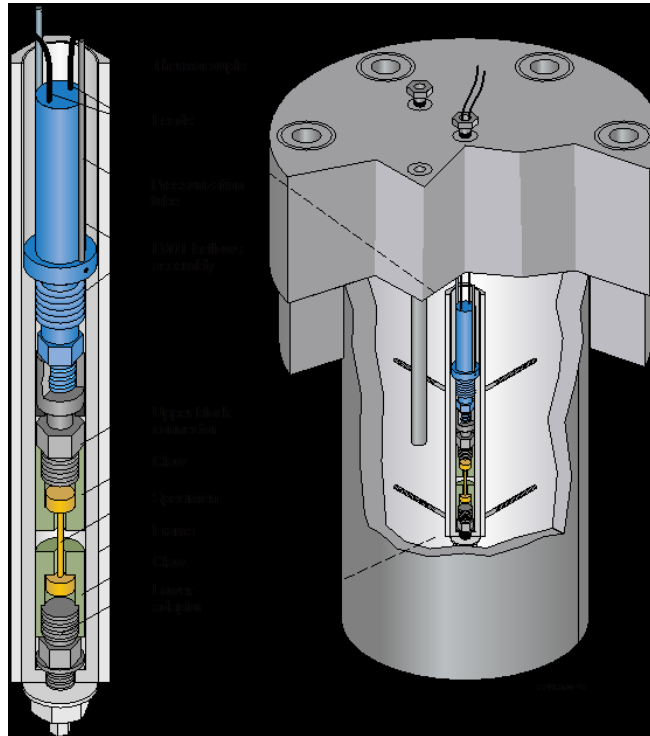


Figure 5. Schematic of the in-pile variable load creep test rig in an autoclave [7].

3.3 Materials

Both types of creep testing specimens were machined out of tight-tolerance multipurpose 6061 aluminum rod that was ½ inch in diameter by 2 feet long. The chemical composition of Al-6061 material is shown in Table 1. The primary motive for selecting aluminum was its low melting temperature (i.e., ~650°C) that fosters accelerated creep testing results. Generally, creep begins at 195–260°C for Al-6061, but at 420–560°C for common stainless steels. Aluminum 6061 isn't a common nuclear alloy used in reactors; however, testing at irradiation creep temperatures (~300°C) of most nuclear materials, without irradiation, wouldn't be creeping at those temperatures. Therefore, to test creep at the relevant temperature, without irradiation, we chose to test a lower temperature alloy (e.g., Aluminum 6061). Additionally, Al-6061 has good mechanical properties, is easy to machine, and remains a very common material for general-purpose use. Traditionally, creep tests last anywhere from 2,000–10,000 hours; however, using materials with much lower melting temperatures can significantly decrease the time to material failure (e.g., 200 hours).

Table 1. Chemical composition for Aluminum 6061.

Chemical Composition (wt. %)	
Chromium	0.05
Copper	0.31
Iron	0.32
Magnesium	0.88
Manganese	0.06
Silicon	0.71
Titanium	0.02
Zinc	0.04
Others	0.15
Al - Balance	97.46

3.4 Creep Testing Specimens

Standard creep specimens were machined in conform with the ASTM E8/E8M-08 standard (10). The standard describes tensile specimens; however, both types of testing, creep and tensile, use this standard specimen requirements. It is crucial that each specimen be proportional, and that the surface finish be smooth and not cold worked by the machining operations. The important part of the specimen is the gauge section (Figure 6). The cross-sectional area of the gauge section is reduced relative to that of the rest of the specimen, such that deformation and failure will be localized in this region. The gauge length, which is the region in

which measurements are taken, is centered within the reduced section. [10] The adjusted gauge length is measured at the 5% offset from the averaged measurement of the diameter.

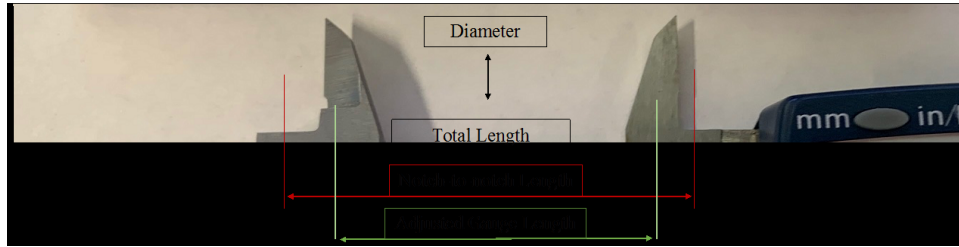


Figure 6. Standard creep specimen.

The out-of-pile creep test rig required a much smaller, simpler creep specimen design than for a standard creep test frame. The creep specimen design for autoclave creep testing is dumbbell-shaped with the reduced section being 3x smaller in diameter than the standard specimen, the claws of which smoothly rest in the grip shoulders. Also, the total length of this specimen is 2.5x smaller than standard; however, the gauge length and total length can still be easily measured, just as with a standard creep specimen. Furthermore, we measured the dumbbell length rather than the notch-to-notch length. The specimen design for the autoclave creep testing is shown in Figure 7.

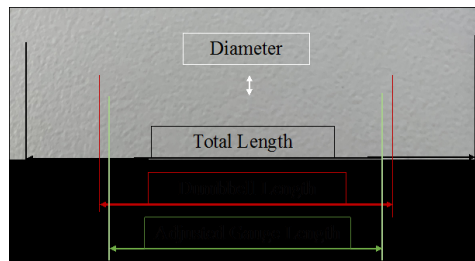


Figure 7. Creep specimen for autoclave creep testing.

3.5 Double Delta

The Double Delta device is designed to most closely assimilate multiphysics (e.g., force, vibration, and thermal) in 3-D reactor environments while remaining extremely controllable and accessible (see Figure 8). Most measurement systems acting in this arena are limited to one of these aspects and lack the breadth to investigate interactive phenomena—especially those encountered in representative 3-D motions/loadings.

The Double Delta device achieves this end by employing two delta platforms to provide 3-D relative motion. The relative motion capability may seem minor when comparing the Double Delta device to a conventional single-platform 3-D system, but this subtle difference is very impactful in terms of workspace efficiency and potential applications, enabling smaller components to be used to achieve the same effect, and also allowing phenomena to be represented as SUB-environments (thermal, water flow, etc.) within the device, rather than having to envelop the device within the target environment—something that leads to many complications/costs.

Additionally, the Double Delta introduces force/torque sensing and control, enabling not only observation of a system's mechanical property behaviors, but also dynamic control over them (e.g., one can replicate flow-induced vibration without water, then control the vibration rather than just observe a few different modes). The device affords a research environment that is a near-twin of an analog reactor environment with a direct digital interface—an environment in which the parameters of interest are manipulated in targeted ways while nullifying the constraints that make direct in-reactor studies inaccessible.

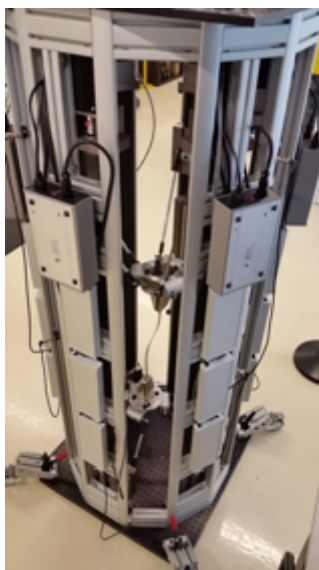


Figure 8. Double Delta system.

4. CALIBRATION RESULTS

4.1 Autoclave Calibration

The LVDT bellow assemblies must be calibrated for the range of temperatures expected during deployment in PWR coolant conditions. This calibration affords the means to relate any measured LVDT demodulation output voltage to a corresponding displacement. Because variable pressure (load) was not required for this creep test, the static load LVDT bellow assembly was used during both the autoclave calibration and autoclave creep testing. Calibration was completed at room temperature and at 100, 200, and 300°C. This temperature range is expected to adequately cover most PWR operating conditions of interest. In this manner, a degree of confidence was achieved relative to the validity of all autoclave testing. Additionally, autoclave testing was conducted in real-time via the NI DAQ system. The full details regarding these calibration efforts and autoclave operations are discussed in [7].

The calibration fixture is assembled by threading the LVDT probe assembly into the LVDT, then threading the travel adapter onto the bottom of the probe assembly, and finally threading the extender onto the bottom of the travel adapter. The assembled components are then lowered into the frame until the flange on the LVDT probe assembly rests on a shoulder internal to the frame. The frame shoulder is

positioned so that the top of the travel limiting recess (Figure 9) is just slightly above the travel block slots in the frame. After the travel blocks are inserted into these slots, the spring and spring plates are stacked on the bottom of the frame and secured via the retaining and lock nut [11]. The autoclave calibration fixture was assembled with the retaining nut tightened just enough to very slightly stretch the bellows and pull the top of the travel limiting recess in the upper block connector into contact with the travel blocks. This is the LVDT's initial position for the autoclave testing, and as the pressure increases, the bellows compresses, altering the LVDT's output demodulation voltage. At a certain autoclave pressure, the bellows ceases compressing, because the travel blocks prevent the upper connector movement that defines the final LVDT output demodulation voltage. The maximum movement of the bellows is 2.29 mm, which will relate to the final LVDT output demodulation voltage.

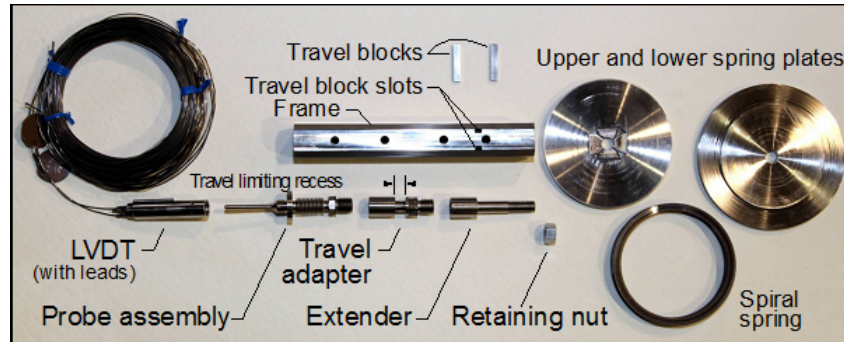


Figure 9. Calibration fixture for autoclave testing.

The maximum workable pressure range for the autoclave is 2,500 psia in a deionized water environment. Results from autoclave calibration tests at room temperature as well as at 100, 200, and 300°C are summarized in Table 2. Autoclave calibration testing confirmed that, for the NI DAQ system, the LVDT signal changes with increasing temperature, which is why target temperature calibration prior to any creep testing is crucial. Since the Al-6061 specimens will be tested at around 300°C, the LVDT sensitivity used for this report is 18.381 V/V per mm (Figure 10).

Table 2. LVDT demodulation sensitivity at room temperature and 100, 200, 300°C.

Temperature (°C)	Sensitivity (V/V/mm rms)
21	16.539
100	16.531
200	17.615
300	18.381

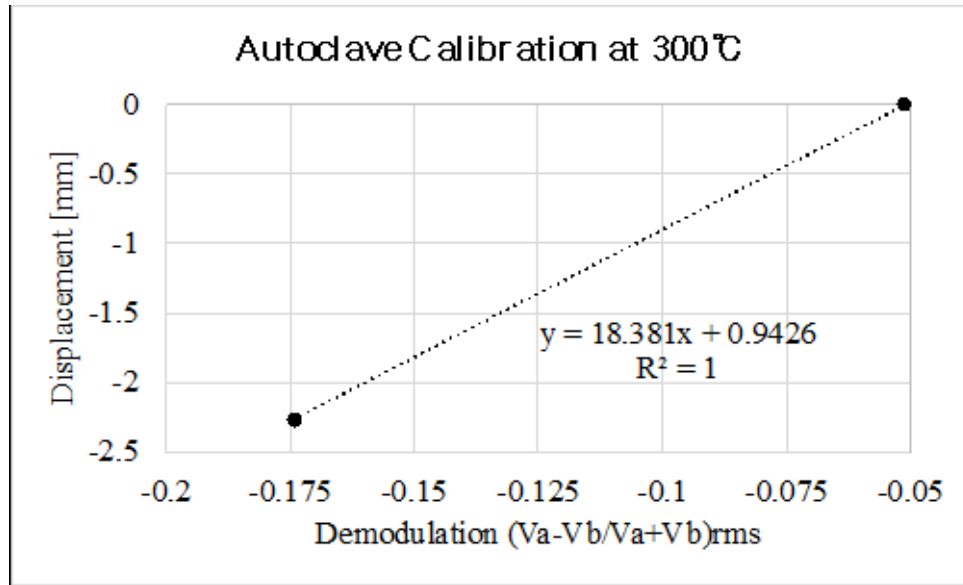


Figure 10. Autoclave calibration testing using the NI DAQ system at 300°C.

4.2 Creep Specimen Measurements

Three Al-6061 standard creep specimens and two dumbbell specimens were measured using a Scherr-Tumico 20-3700 optical comparator with MetLogix M2 measurement software. Table 3 shows, for both types of creep specimens, all the measurements taken prior to any creep testing, using both standard and autoclave testing.

Table 3. All Al-6061 creep specimen measurements prior to creep testing.

Creep Specimen Type	Specimen Number	Type of Measurement (mm)					
		Total Length	Notch-to-Notch Length				
			Measurement 1	Measurement 2	Measurement 3	Measurement 4	
Standard	1	99.07	42.931	42.939	42.936	42.936	
			Average	42.9355			
			Diameter				
			Measurement 1	Measurement 2	Measurement 3	Measurement 4	
			6.351	6.351	6.347	6.347	
			Average	6.349			
			Adjusted Gauge Length				
			Measurement 1	Measurement 2	Measurement 3	Measurement 4	
			34.094	34.257	34.159	34.216	
			Average	34.1815			
Creep Specimen Type	Specimen Number	Type of Measurement (mm)					
		Total Length	Notch-to-Notch Length				
			Measurement 1	Measurement 2	Measurement 3	Measurement 4	
Standard	2	99.15	42.923	42.926	42.919	42.924	
			Average	42.923			
			Diameter				
			Measurement 1	Measurement 2	Measurement 3	Measurement 4	
			6.359	6.36	6.358	6.355	
			Average	6.358			

			Adjusted Gauge Length			
			Measurement 1	Measurement 2	Measurement 3	Measurement 4
			34.227	34.265	34.194	34.212
			Average	34.2245		
Creep Specimen Type	Specimen Number	Type of Measurement (mm)				
		Total Length	Notch-to-Notch Length			
			Measurement 1	Measurement 2	Measurement 3	Measurement 4
			42.926	42.924	42.916	42.927
			Average	42.92325		
			Diameter			
			Measurement 1	Measurement 2	Measurement 3	Measurement 4
			6.345	6.347	6.345	6.346
			Average	6.34575		
Adjusted Gauge Length						
Measurement 1	Measurement 2	Measurement 3	Measurement 4			
34.217	34.233	34.212	34.154			
Average	34.204					
Creep Specimen Type	Specimen Number	Type of Measurement (mm)				
		Total Length	Diameter			
			Measurement 1	Measurement 2	Measurement 3	Measurement 4
			2.039	2.036	2.033	2.031
			Average	2.03475		
			Adjusted Gauge Length			
			Measurement 1	Measurement 2	Average	
			26.632	26.646	26.639	
			Dumbbell Length			
Measurement 1	Measurement 2	Average				
28.046	28.039	28.0425				
Creep Specimen Type	Specimen Number	Type of Measurement (mm)				
		Total Length	Diameter			
			Measurement 1	Measurement 2	Measurement 3	Measurement 4
			2.033	2.035	2.034	2.033
			Average	2.03375		
			Adjusted Gauge Length			
			Measurement 1	Measurement 2	Average	
			26.672	26.63	26.651	
			Dumbbell Length			
Measurement 1	Measurement 2	Measurement 3	Measurement 4			
28.066	28.058	28.058	28.031			
Average	28.05325					

5. CREEP TESTING RESULTS

5.1 Standard Creep Testing

The first Al-6061 specimen was used to learn whether the actual rupture time was comparable to the predicted rupture time estimated via the Larson-Miller parameter method. The aim was to find a specific temperature and stress combination that, when applied to Al-6061 specimens, would lead to a rupture

time of around 2 weeks (336 hours). A temperature of 345°C and a stress of 16.86 MPa were first suggested based on the Larson-Miller parameter method; however, the actual rupture time ended up being ~54 hours. Therefore, the next two specimens were tested at much higher predicted rupture time estimates using the Larson-Miller parameter method. A final temperature of 325°C and a stress of 16 MPa were chosen for Al-6061 specimens #2 and #3. In Figure 11, which shows the creep curve for Al-6061 specimen #2, the primary creep is very fast, followed by a secondary steady-state creep rate of 0.004% strain per hour. The tertiary creep stage is also very rapid, with failure of the sample occurring at ~210 hours.

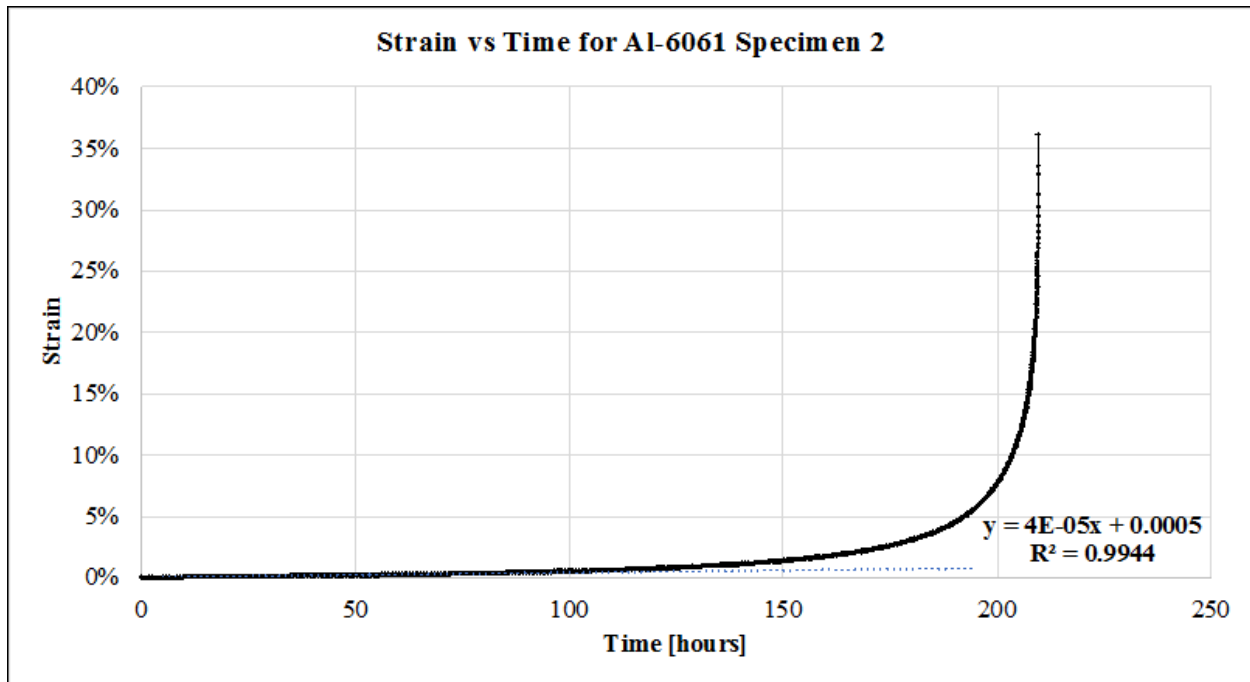


Figure 11. Creep curve for Al-6061 specimen #2.

Figure 12 shows the creep curve for Al-6061 specimen #3, and it is almost identical to the one for specimen #2. The secondary steady-state creep rate is 0.004% strain per hour, just as for sample #2. The tertiary creep stage is also very rapid, with failure of the sample occurring at ~207 hours.

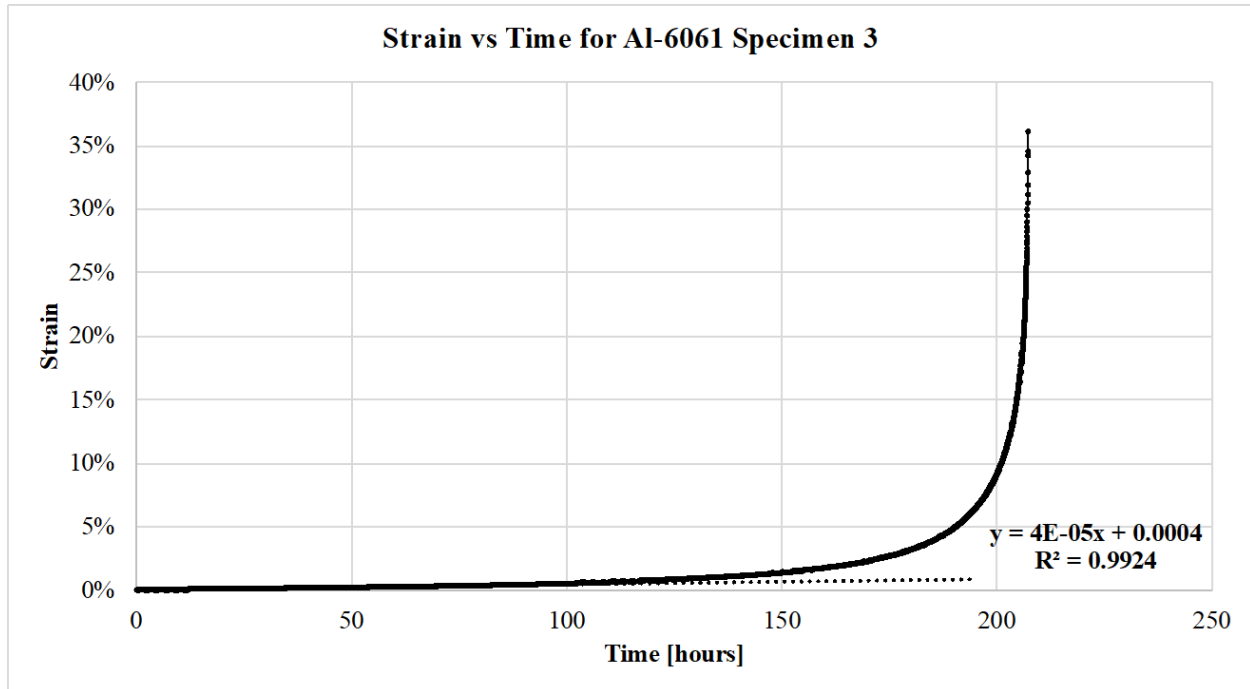


Figure 12. Creep curve for Al-6061 specimen #3.

5.2 Standard Creep Specimens

As expected, all the Al-6061 standard specimens failed by breaking within the gauge length region; however, each sample broke at different points within that region. Since aluminum is a ductile metal, standard specimen #2 had to be cut off at the shoulder grip after getting stuck in the creep testing frame. Thus, for creep specimen #2 (Figure 13), it was impossible to measure the total length post-testing.



Figure 13. Al-6061 creep specimen #2 after standard creep testing at 325°C and 15.896 MPa.



Figure 14. Al-6061 creep specimen #3 after standard creep testing at 325°C and 15.896 MPa.

Table 4 represents the total and notch-to-notch length measurements taken both before and after creep testing. Both LVDTs measured a total average elongation of 12.37 mm for specimens #2 and #3; however, specimen #3 showed a much larger change in its total and notch-to-notch lengths, at an average

of 16.66 mm (Table 4). This could be due to the commercial LVDTs not recording the last few seconds of strain measurements prior to specimen failure, as the recording time interval was every 60 seconds (1 minute).

Table 4. Length measurements, before and after standard creep testing.

Sample ID	Total Length (mm)			Notch-to-Notch Length (mm)			Average Delta (mm)
	Before	After	Delta	Before	After	Delta	
Standard 2	99.15	N/A	-	42.923	55.35	12.427	12.427
Standard 3	99.11	115.67	16.56	42.923	59.68	16.757	16.659

5.3 Autoclave Creep Testing

The following main autoclave creep testing objectives were met:

- Test creep rig verification to ensure it can withstand elevated temperatures, pressures, long working hours (36 days) as a robust system
- Verification of signal processing equipment using the NI DAQ system, and no data loss over a duration of 36 days
- Gain insights from lessons learned that can be applied when finalizing the design prior to deployment in the Materials Test Reactor.

To address the first two objectives, an Al-6061 creep specimen with a gauge diameter of 2.04 mm and a dumbbell length of 28.04 mm was loaded into the creep test rig inside the autoclave (see Figure 7). Instrument indications for temperature and LVDT output demodulation voltage were noted using the NI DAQ system, while the autoclave temperature and pressure remained at normal. The autoclave temperature and pressure were then gradually increased before ultimately being stabilized at 325°C and 2,300 psi (15.86 MPa). The corresponding instrument indications for temperature and LVDT output demodulation voltage were again noted using the NI DAQ. When the autoclave stabilized, the NI DAQ system was used to record, at 60-second (1-minute) intervals, the LVDT output demodulation voltage and TC signal for ~36 days. The results are shown in Figure 15.

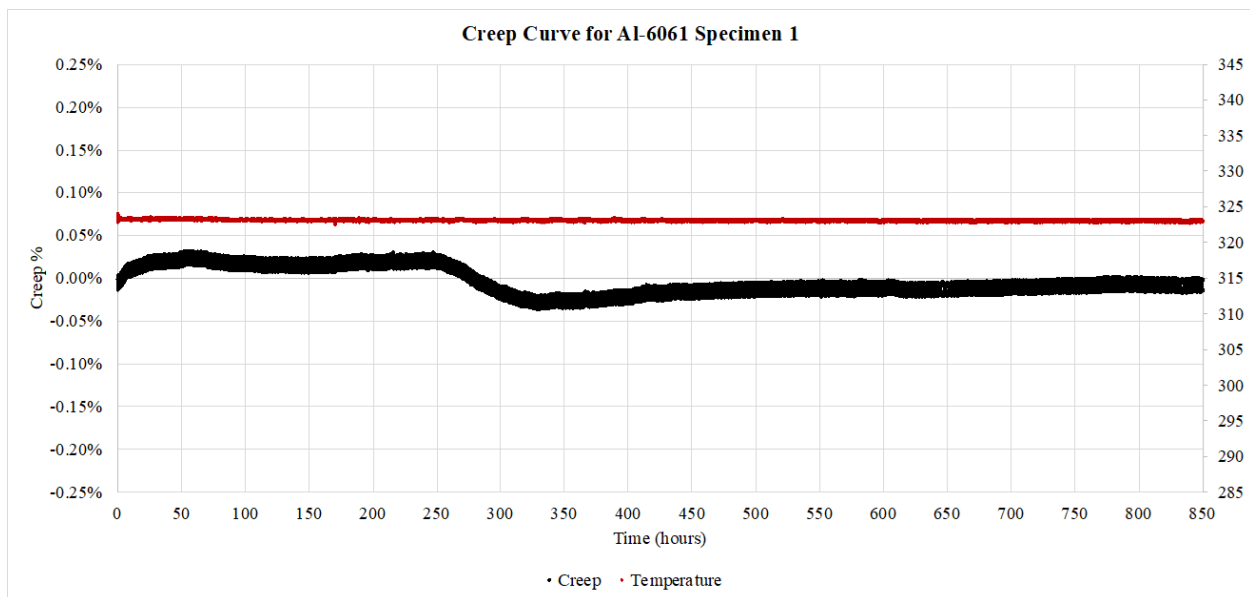


Figure 15. Autoclave creep curve for Al-6061 dumbbell specimen #1.

Unfortunately, when the test ended, Al-6061 dumbbell specimen #1 was fully oxidized and no longer intact in the creep test rig, as shown in Figure 16. Thus, it is unknown how fast the Al-6061 specimen began oxidizing in the autoclave. As a result, the creep curve results in Figure 15 are inconclusive. Furthermore, the deionized water in the autoclave was not chemically controlled to prevent oxidization from occurring.

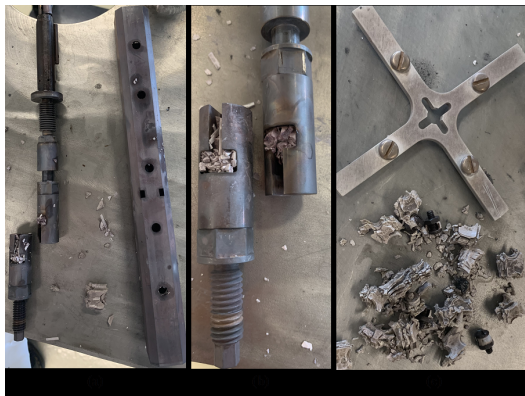


Figure 16. Dumbbell specimen #1 after autoclave creep testing at 325°C and 15.896 MPa: (a) the creep test rig with oxidized specimen #1, (b) the creep test rig claws holding the remaining pieces of dumbbell specimen #1, and (c) the LVDT cable holder (also made from aluminum) before (top) and after (bottom) autoclave creep testing oxidation.

6. CONCLUSION

As part of the Nuclear Energy Enabling Technology's Advanced Sensor and Instrumentation program, an instrumented creep testing capability was developed by the HTTL team to enable specimens (e.g., Al-6061) to be tested under prototypic PWR conditions (e.g., 325°C and 2300 psi). Results from the autoclave evaluations demonstrated even the worst-case scenario of having the specimen completely disintegrate, while still being able to record and maintain the system at steady state conditions indicating that robust system construction of the test rig was a success. These lessons learned will be used to finalize recommendations for an enhanced design that will be inserted into the flowing autoclave. Although the INL-developed creep testing capability will ultimately be applied to a wide range of materials, initial efforts focused on aluminum 6061 verification testing. In summary, testing of the INL creep test rig confirmed its availability and robustness for deployment, as well as its ability to partially replace those testing capabilities lost due to the termination of HBWR operations.

7. FUTURE WORK

The first lesson learned from this work is that autoclave testing requires either a dry environment (inert gas) testing capability or a chemically controlled water flow capability to prevent any oxidization issues from arising in the creep specimens. Additionally, stress relaxation measurements would broaden the in-pile test rig capability for future work. LVDTs supplied by the Institute for Energy Technology and the Halden Reactor Project are not sustainable long-term; therefore, looking into the use of strain gauges, printed strain gauges, or other small strain measuring devices would greatly benefit and broaden the capabilities for multi-sensor and multi-specimen in-pile testing. Finally, incorporating the Double Delta system to be able to test mechanical sensors, such as strain gauges, in multiaxial stress/strain environments would benefit the mechanical testing capability.

8. REFERENCES

1. Sun, C., et al. 2015. "Superior Radiation-Resistant Nanoengineered Austenitic 304L Stainless Steel for Applications in Extreme Radiation Environments." *Scientific Reports* 5(1). doi:10.1038/srep07801.

2. Singh, B. N., et al. 2003. "In-Reactor Uniaxial Tensile Testing of Pure Copper at a Constant Strain Rate at 90°C." *Journal of Nuclear Materials* 320(3): 299–304. doi: 10.1016/S0022-3115(03)00234-4.
3. Davis, K. L., D. L. Knudson, J. L. Rempe, J. C. Crepeau and S. Solstad. 2015. "Design and Laboratory Evaluation of Future Elongation and Diameter Measurements at the Advanced Test Reactor." *Nuclear Technology* (191): 92-105. doi: 10.13182/NT14-60.
4. Kim, B. G., J. L. Rempe, D. L. Knudson, K. G. Condie, and B. H. Sencer. 2010. "In-Situ Creep Testing Capability Development for the Advanced Test Reactor." INL/EXT-10-17779, Idaho National Laboratory.
5. Knudson, D. L. and J. L. Rempe. 2012. "Linear Variable Differential Transformer Based Elongation Measurements in Advanced Test Reactor High Temperature Irradiation Testing." *Measurement Science and Technology* 23 (2): 025604. doi: 10.1088/0957-0233/23/2/025604.
6. Kim, B. G., et al. 2019. "In-Situ Creep Testing Capability for the Advanced Test Reactor." *Nuclear Technology* 179 (3): 417–428 doi: 10.13182/nt12-a14173.
7. Wilding, M. A., et al. 2020. "Out-of-Pile Test of LVDT-Based Creep Test Rig at PWR Prototypical Conditions." INL/EXT-20-60037, Idaho National Laboratory.
8. "ASTM e139 - 11(2018)." ASTM International - Standards Worldwide, <https://www.astm.org/Standards/E139.htm>.
9. Mathers, G. "Creep and Creep Testing." *TWI*, Accessed 09.30.2021:<https://www.twi-global.com/technical-knowledge/job-knowledge/creep-and-creep-testing-081/?vAction=swpTextOnly>.
10. "ASTM E8/E8M-08 Standard Test Methods for Tension Testing of Metallic Materials." *ASTM International - Standards Worldwide*, Accessed 09.30.2021: <https://www.astm.org/DATABASE.CART/HISTORICAL/E8E8M-08.htm>.
11. Davis, K. L., et al. 2013. "A Variable Load LVDT-Based Creep Test Rig for Use in ATR Loop 2A." INL/EXT-13-29551, Idaho National Laboratory.